Magnetic polarisation effects of temperature sensors and heaters in *LISA* Pathfinder

To cite this article: J Sanjuán *et al* 2009 *J. Phys.: Conf. Ser.* **154** 012001

Magnetic polarisation effects of temperature sensors and heaters in *LISA* Pathfinder

J Sanjuán[1,2], A Lobo[1,2], M Nofrarias[3], J Ramos-Castro[4], N Mateos[1,2] and X Xirgu[1,2]

[1] Institut de Ciències de l'Espai, *CSIC*, Facultat de Ciències, Torre C5 parell, 08193 Bellaterra, Spain
[2] Institut d'Estudis Espacials de Catalunya (*IEEC*), Edifici Nexus, Gran Capità 2-4, 08034 Barcelona, Spain
[3]Max-Planck-Institut für Gravitationsphysik (Albert-Einstein-Institut), Callinstrasse 38, D-30167 Hannover, Germany
[4]Departament d'Enginyeria Electrònica, *UPC*, Campus Nord, Edifici C4, Jordi Girona 1-3, 08034 Barcelona, Spain

E-mail: `sanjuan@ieec.fcr.es`

Abstract. Temperature sensors and heaters belong in the diagnostics subsystem of the *LISA* Technology Package (*LTP*) on board *LISA* Pathfinder, the technology demonstrator for *LISA*. A number of these diagnostics items are placed at short distances from the *LTP* proof masses, and are negative temperature coefficient (*NTC*) thermistors. By design, these devices have tiny amounts of ferromagnetic materials which therefore constitute a potential source of disturbance to the performance of the *LTP*. We present a detailed magnetic characterisation of the *NTC*'s, and use the data to evaluate their impact on the acceleration noise budget of the *LTP*. The effect is seen to be small, and can be further reduced if the *NTC*'s are submitted to a de-magnetisation process before they are attached. Re-magnetisation is unlikely, as rather strong fields (mili-Tesla) are required to re-magnetise the *NTC*'s

1. Introduction

LISA Pathfinder [1] is a technological mission intended to demonstrate that two proof masses can be put into free-fall to a certain level of accuracy. This idea is reflected in the differential acceleration noise requirement for the *LTP*

$$S_{\delta a}^{1/2}(\omega) \leq 3\times 10^{-14}\left[1+\left(\frac{\omega/2\pi}{3\,\mathrm{mHz}}\right)^2\right]\,\mathrm{m\,s^{-2}\,Hz^{-1/2}} \tag{1}$$

in the frequency band between 1 mHz to 30 mHz.

This requirement implies stringent limitations on *internal* environment fluctuations. Specifically, thermal and magnetic fluctuations must be very low not to exert any noise force on the test masses (*TM*'s) [2].

The diagnostics subsystem [3] responsible of measuring such low temperature fluctuations includes 8 thermistors[1] (4 as temperature sensors and 4 as heaters) surrounding each of the

[1] BetaTherm thermistors.

TM's. Thermistors are manufactured mixing and synthesising oxides doped with ferromagnetic materials [4] which make them potentially dangerous as they are placed close[2] to the *TM*'s —see figure 1— since magnetic field and magnetic field gradient in the *TM* translate into a force due to its non-zero susceptibility and remanent magnetic moment —see section 2.

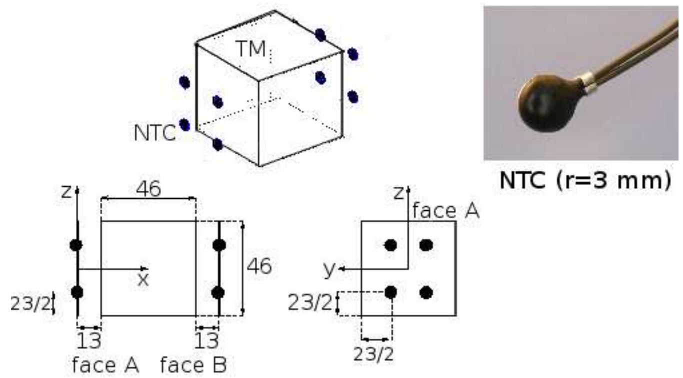

Figure 1. Situation of the thermistors surrounding the *TM*. Units in mm.

The *LTP* noise acceleration budget assigned to magnetic effects in the *TM* is [5]

$$S^{1/2}_{\delta a,\,\mathrm{magn}}(\omega) \leq 12\,\mathrm{fm\,s^{-2}\,Hz^{-1/2}} \tag{2}$$

in the measurement bandwidth (*MBW*). For this reason magnetic field, magnetic field gradient and their fluctuations must be well kept under a certain limits. The presence of the *NTC*'s might add noticeable noise to the differential acceleration. This paper describes the steps performed in order to quantify this effect. It is organised as follows: in section 2 the expression of the acceleration noise as a function of the magnetic field and magnetic field gradient is given together with the nominal properties of the *TM* and background magnetic conditions. Section 3 shows the the measured hysteresis curve of the thermistors. Section 4 describes the numerical calculations performed to obtain the magnetic field and magnetic field gradient in the *TM* considering the 8 *NTC*'s surrounding it. Section 5 shows the measurement of the first magnetisation curve (*FMC*) of the thermistors. Section 6 details the excess acceleration noise caused by the presence of the *NTC*'s surrounding the *TM*. Finally, in section 6 the conclusions are given.

2. Force fluctuations in the *TM* due to magnetic issues

The force fluctuation due to magnetic effects is [6]:

$$\begin{aligned} S_{\delta F_x}(\omega) &= V^2|\langle\mathbf{M}\rangle|^2 S_{\nabla B_x}(\omega) + \left(\frac{\chi V}{\mu_0}\right)^2 |\langle\boldsymbol{\nabla} B_x\rangle|^2 S_{\mathbf{B}}(\omega) + \\ &\quad + \left(\frac{\chi V}{\mu_0}\right)^2 |\langle\mathbf{B}\rangle|^2 S_{\nabla B_x}(\omega) \end{aligned} \tag{3}$$

where V is the *TM* volume, $\mathbf{M}$ is the remanent magnetisation of the *TM*, χ is the magnetic susceptibility of the *TM*, $\langle\mathbf{B}\rangle$ is the magnetic field average over the *TM* volume and $\langle\boldsymbol{\nabla} B_x\rangle$ the same for the magnetic field gradient. $S_{\mathbf{B}}$ and $S_{\nabla B_x}$ are the magnetic field and magnetic field gradient fluctuations over the *TM*[3]. The nominal values for these parameters are [1]:

[2] The distance from the sensors to the closer face of the *TM* is 13 mm.
[3] Assuming the fluctuations are homogeneous in all the *TM* volume.

- *TM* magnetic properties: $|\chi| = 10^{-5}$ and $\mathbf{M}$=10^{-4} A m^{-1},
- Background *dc* values: $|\mathbf{B}_{\rm bg}| \leq$ 10 μT and $|\boldsymbol{\nabla} B_{{\rm bg},\,x}| \leq 5\sqrt{3}\,\mu$T m^{-1},
- Magnetic fluctuation values: $S^{1/2}_{\mathbf{B}}(\omega) \leq$650 nT Hz$^{-1/2}$ and $S^{1/2}_{\nabla B_x}(\omega) \leq 250\sqrt{3}$ nT m^{-1} Hz$^{-1/2}$ in the frequency band from 1 mHz to 30 mHz[4]

By using these values and equation (3) the noise acceleration due to the magnetic effects in the absence of thermistors is calculated and shown in table 1.

Table 1. Foreseen differential acceleration noise in the *LTP* due to magnetic effects in the *TM* (in the absence of thermistors).

Term	$S_{\Delta a_x}$ [fm s^{-2} Hz$^{-1/2}$]
$V\lvert\langle\mathbf{M}\rangle\rvert S^{1/2}_{\boldsymbol{\nabla} B_x}(\omega)$	2.15
$(\chi V/\mu_0)\lvert\langle\boldsymbol{\nabla} B_x\rangle\rvert S^{1/2}_{\mathbf{B}}(\omega)$	2.22
$(\chi V/\mu_0)\lvert\langle\mathbf{B}\rangle\rvert S^{1/2}_{\nabla B_x}(\omega)$	1.70
$S^{1/2}_{\rm total\ mag}(\omega)$	4.46

The presence of the thermistors implies that

$$\mathbf{B} = \mathbf{B}_{\rm background} + \mathbf{B}_{NTC} \tag{4}$$

and, thus, the effect of $\mathbf{B}_{NTC}$ (and its associated gradient) in the *TM* acceleration needs to be quantified.

3. *NTC*'s magnetic characterisation: the hysteresis curve

The hysteresis curve for a set of thermistors is shown in figure 2. The measurement was performed by using a SQUID (Quantum Design MPMS XL Squid) at the Serveis Científico-Tècnics of the Universitat de Barcelona [7, 8].

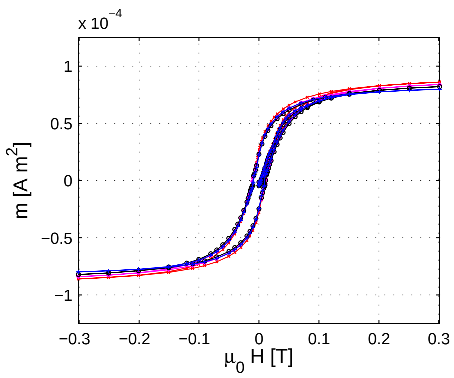

Figure 2. Hysteresis curve at 300 K for the set (four samples) of 10 kΩ *NTC* thermistors of BetaTherm.

The relevant information that can be extracted from figure 2 is shown in table 2.

[4] These values are superseded.

Table 2. Magnetic properties of the BetaTherm *NTC* thermistors. (i) $|\mathbf{m}_\mathrm{r}|$ is the remanent magnetic moment after saturation and at zero magnetic field, (ii) $|\mathbf{m}_\mathrm{sat}|$ is the magnetic moment at the saturating magnetic field and (iii) $\mu_0|\mathbf{H}_\mathrm{coer}|$ is the coercive field.

$\|\mathbf{m}_\mathrm{r}\|$	$\|\mathbf{m}_\mathrm{sat}\|$	$\mu_0\|\mathbf{H}_\mathrm{coer}\|$
$24\pm2\,\mu$A m^2	$83\pm2.5\,\mu$A m^2	10 mT

4. Numerical calculations

Numerical calculations to obtain the average magnetic field, $\langle\mathbf{B}\rangle$, and the average magnetic field gradient, $\langle\nabla B_x\rangle$, considering the 8 *NTC*'s surrounding the *TM* have been performed assuming: (i) *NTC*'s behave like magnetic dipoles and (ii) the remanent magnetic moment is the one measured after *NTC* magnetic saturation[5].

Calculations considering different orientations of the 8 magnetic moments of the *NTC*'s allow us to know the worst possible combinations. A simple scheme of the magnetic moment orientations (arrows in the figure) surrounding the *TM* and the numerical values obtained are given in figure 3 and table 3.

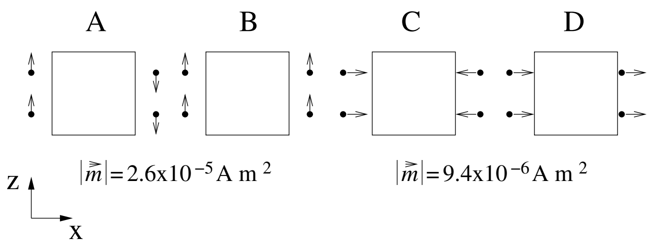

Figure 3. Configuration analysed for the magnetic field and magnetic field gradient calculations. This four configurations cover the worst cases involved in the problem. Intermediate configurations lead to smaller values of the magnetic field and magnetic field gradient in the *TM*. Arrows stand for the *NTC*'s magnetic moment orientation [6].

Table 3. Average value modulus of the magnetic field and magnetic field gradient caused by the eight *NTC*'s in the *TM* using a remanent magnetic moment of 24 μA m^{-2}.

Conf.	$\|\langle\mathbf{B}\rangle\|$ [μT]	$\|\langle\nabla B_x\rangle\|$ [μT m^{-1}]
A	0	15.5
B	0.25	0
C	0	11.3
D	0.18	0

Graphical representations of the magnetic field and magnetic field gradient in the *TM* volume are shown in figure 4.

[5] This is a very worst case scenario since exposing the thermistors to their saturating magnetic field ($\approx$0.3 T) is unlikely.

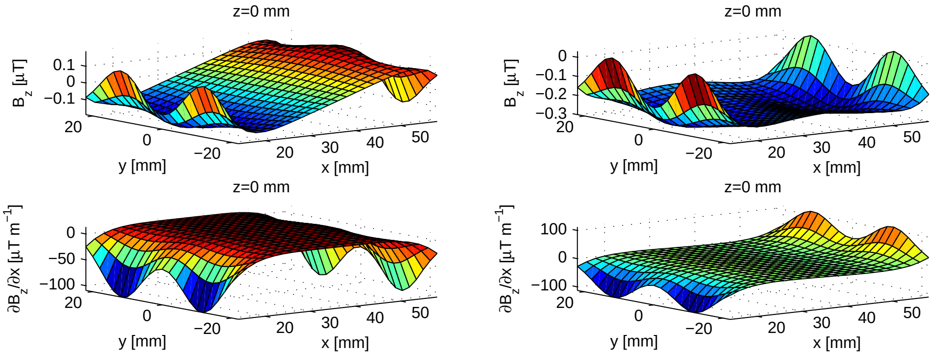

Figure 4. Representation of the z-component of the magnetic field and magnetic field gradient in the equatorial plane of *TM*. Left: Configuration A (see figure 3). Right: Configuration B (see figure 3).

5. *NTC*'s first magnetisation curve (*FMC*)

The numbers obtained in section 4 are very pessimistic since the magnetic field and magnetic field gradient have been calculated using the remanent magnetic moment, $|\mathbf{m}_{\rm r}|$, after saturating the *NTC*'s. To obtain more realistic estimations, the *FMC* was measured. The *FMC* consists in measuring the magnetic moment vs. applied field relationship after the de-magnetisation of the item [9]. The *FMC* is shown in figure 5 [7, 8].

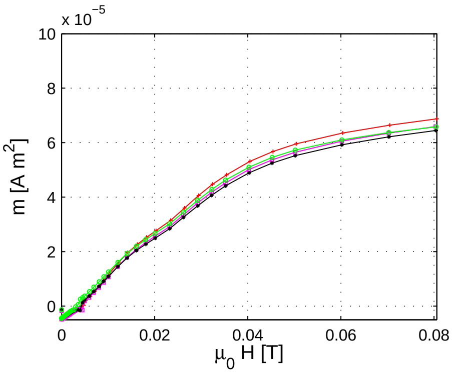

Figure 5. Measured *FMC* for a set of BetaTherm thermistors.

The remanent magnetic moment measured after the de-magnetisation is:

$$|\mathbf{m}_{\rm demag}| = 1.4 \pm 0.2 \; [\mu{\rm A\,m^2}] \tag{5}$$

which is about one order of magnitude less than the one measured after saturating the thermistor.

The *FMC* for the *NTC*'s can be linearised near the de-magnetisation zone as —see figure 5:

$$|\mathbf{m}_{\rm FMC,\,BetaTherm}| \simeq 1.45\times 10^{-3}\,\mu_0\,|\mathbf{H}_{\rm FMC}| \tag{6}$$

This relationship will be useful for calculations of the maximum magnetic field the *NTC*'s can be exposed in order not to increase the acceleration noise —see section 6.

6. Excess *TM* noise calculations

The acceleration noise for three different scenarios will now be calculated and compared. The analysed scenarios are:

- absence of thermistors
- presence of thermistors with the maximum possible remanent magnetic moment, i.e., after saturation, $|\mathbf{m}_\mathrm{r}| = 24\,\mu\mathrm{A\,m}^{-2}$,
- presence of thermistors after de-magnetisation, $|\mathbf{m}_\mathrm{demag}| = 1.4\,\mu\mathrm{A\,m}^{-2}$.

The numbers obtained are summarised in table 4.

Table 4. Acceleration noise for three different scenarios. Units: $\mathrm{fm\,s^{-2}\,Hz^{-1/2}}$. Δ stands for the increase of the noise with respect to the "NO NTC's" noise numbers. The frequency band is between 1 mHz and 30 mHz.

Term	No NTC's	$\lvert\mathbf{m}_\mathrm{r}\rvert=$ $26\,\mu\mathrm{A\,m}^2$	$\lvert\mathbf{m}_\mathrm{demag}\rvert=$ $1.4\,\mu\mathrm{A\,m}^2$
$V\lvert\langle\mathbf{M}\rangle\rvert S^{1/2}_{\boldsymbol{\nabla} B_x}(\omega)$	2.10	2.10	2.10
$(\chi V/\mu_0)\lvert\langle\boldsymbol{\nabla} B_x\rangle\rvert S^{1/2}_{\mathbf{B}}(\omega)$	2.22	6.12	2.44
$(\chi V/\mu_0)\lvert\langle\mathbf{B}\rangle\rvert S^{1/2}_{\nabla B_x}(\omega)$	1.70	1.70	1.70
$S^{1/2}_{\mathrm{total\ mag}}(\omega)$	4.45	7.29	4.54
Δ	—	64%	2%

If a desired Δ is chosen then the maximum magnetic field that the thermistors can tolerate can be calculated using equation 6. For instance, if $\Delta < 10\%$ is required, the thermistors should be de-magnetised and not exposed to magnetic fields higher than 5 mT.

7. Conclusions

The investigations carried out with respect to the magnetic characteristics of the *NTC*'s and their impact on the performance of the *LTP* experiment are the following:

- *NTC*'s show ferromagnetic behaviour.
- The magnetic properties of the *NTC*'s can degrade the performance of the *LTP*, increasing the magnetic noise by $\sim 65\,\%$ relative to the background in the very worst possible situation. However, even in such extreme conditions the budgeted magnetic noise ($12\,\mathrm{fm\,s^{-2}}/\sqrt{\mathrm{Hz}}$) is not reached.
- de-magnetisation of the *NTC*'s produces very good results: the magnetic noise can be reduced by about an order of magnitude, which makes it mostly negligible.

Acknowledgments

Support for this work came from Project ESP2004-01647 of Plan Nacional del Espacio of the Spanish Ministry of Education and Science (MEC). JS acknowledges a grant from MEC.

References

[1] Vitale S 2005 Science Requirements and Top-level Architecture Definition for the LISA Technology Package (*LTP*) on Board *LISA* Pathfinder (SMART-2), report no. LTPA-UTN-ScRD-Iss003-Rev1
[2] Araújo H *et al* 2007 *Journal of Physics: Conference Series* **66** 012003

[3] Sanjuán J, Lobo A, Nofrarias M, Ramos-Castro J and Riu P 2007 *Rev Sci Instr* **78** 104904
[4] Pallàs R and Webster JG 2000 *Sensors and signal conditioning* (New York)
[5] Vitale S *et al* 2005 Science requirement and top-level architecture definition for the *LISA* Technology Package (*LTP*) on board *LISA* Pathfinder LTPA-UTN-ScRD Issue 3.1
[6] Sanjuán J *et al* 2008 *Rev Sci Instr* **79** 084503
[7] Nofrarias M and Sanjuán J 2007 Magnetic characterisation of thermal diagnostic items S2-IEC-TN-3036
[8] Sanjuán J and Nofrarias M 2008 Characterisation and impact of NTC magnetic properties on the LTP noise budget S2-IEC-TN-3038
[9] Sears FW and Zemansky MW 1991 *College physics* (MA)